

Dalton Transactions

Accepted Manuscript



This is an *Accepted Manuscript*, which has been through the Royal Society of Chemistry peer review process and has been accepted for publication.

Accepted Manuscripts are published online shortly after acceptance, before technical editing, formatting and proof reading. Using this free service, authors can make their results available to the community, in citable form, before we publish the edited article. We will replace this *Accepted Manuscript* with the edited and formatted *Advance Article* as soon as it is available.

You can find more information about *Accepted Manuscripts* in the [Information for Authors](#).

Please note that technical editing may introduce minor changes to the text and/or graphics, which may alter content. The journal's standard [Terms & Conditions](#) and the [Ethical guidelines](#) still apply. In no event shall the Royal Society of Chemistry be held responsible for any errors or omissions in this *Accepted Manuscript* or any consequences arising from the use of any information it contains.

Cite this: DOI: 10.1039/c0xx00000x

www.rsc.org/xxxxxx

ARTICLE TYPE

Cyclometallated platinum(II) complexes of benzylidene-2,6-diisopropylphenylamine containing bidentate phosphines: Synthesis, structural properties and reactivity studies

Feng Zheng^{a,c}, Alan T. Hutton^a, Cornelia G.C.E. van Sittert^b, Wilhelmus J. Gerber^c and Selwyn F. Mapolie^{*c}

Received (in XXX, XXX) Xth XXXXXXXXX 20XX, Accepted Xth XXXXXXXXX 20XX

DOI: 10.1039/b000000x

The reaction of the cyclometallated complex [PtCl(N[^]C)(dmsO)] **1**, (N[^]C represents the cyclometallated Schiff base, benzylidene-2,6-diisopropylphenylamine), with 1,1-bis(diphenylphosphino)ferrocene, dppf, 1,1-bis(diphenylphosphino)methane, dpmm, and 1,2-bis(diphenylphosphino)ethane, dppe, in a 2:1 ratio or an equimolar ratio using acetone as solvent produced the corresponding binuclear and mononuclear diphosphines platinum complexes. In the case of the mononuclear complexes, the diphosphines act as either a bidentate [N[^]C] ligand or a monodentate [N[^]C-κ1C] ligand depending on the size of bite angle of diphosphines, while in the case of the binuclear complexes, the diphosphines acts as a bridging ligand between the two metal centres. The solid state structures of some the binuclear as well as mononuclear species are reported. The mononuclear derivatives were found to show different behaviour in solution and in the solid state when compared to the binuclear analogues. This behaviour is also influenced by the nature of the diphosphines ligands employed.

1. Introduction

Cyclometallated platinum compounds are of great interest due to their useful applications in many fields.¹ Since *cis*-[PtCl₂(dmsO)₂] has been shown as an useful substrate for direct cycloplatination, the coordination behaviour of N-benzylidenebenzylamines as cyclometallating ligands with *cis*-[PtCl₂(dmsO)₂] were recently reported.² The labile dmsO group can easily be replaced by other ligands, including phosphine ligands, leading to more thermally stable cyclometallated platinum complexes.

Bidentate phosphines (diphosphines) are an important class of tertiary phosphine ligands in organometallic chemistry and have found wide applications.³ In general; diphosphines are versatile and robust ligands that are known to have different coordination ability. Reactions of the platinum(II) sulfoxide complex with diphosphine ligands give either dinuclear species, with bridging phosphines,^{4,5} or mononuclear species with chelating phosphines,^{2a,4b} respectively. The cyclometallated platinum complexes based on diphosphine ligands have for example shown photophysical properties^{4a} and antitumor activities.^{4c,6}

A preliminary study conducted by us has found that the cyclometallated palladium complexes containing N-benzylidenebenzylamine and diphosphine ligands exhibit promising antitumor activities. The series of platinum analogues presented here could thus also potentially be biological active. The screening of these platinum complexes for their anti-cancer behaviour is currently being conducted. In an attempt to better

understand these cyclometallated platinum(II) complexes, we wanted to first study the diversity of the chemistry of these complexes before pursuing further work with possible applications.

Upon reaction with phosphines, the tendency of cyclometallated palladium and platinum compounds to undergo cleavage of the metal–nitrogen bond has been taken as a metallacycle stability criterion.⁷ In order to gain insight into the factors responsible for the cleavage of the metal–nitrogen bond, the reactions of the (N[^]C) cycloplatinated sulfoxide complex with diphosphines which have different bite angles, i.e., dpmm, dppe and dppf, were undertaken. The present work is focused on two issues: (1) an evaluation of the effect of bite angle of three diphosphines on the nature of the platinacycles formed, in which the diphosphines act as either chelating or bridging ligands, (2) a comparative analysis of structural and various properties of these monomeric and dimeric platinacycles.

2. Results and Discussion

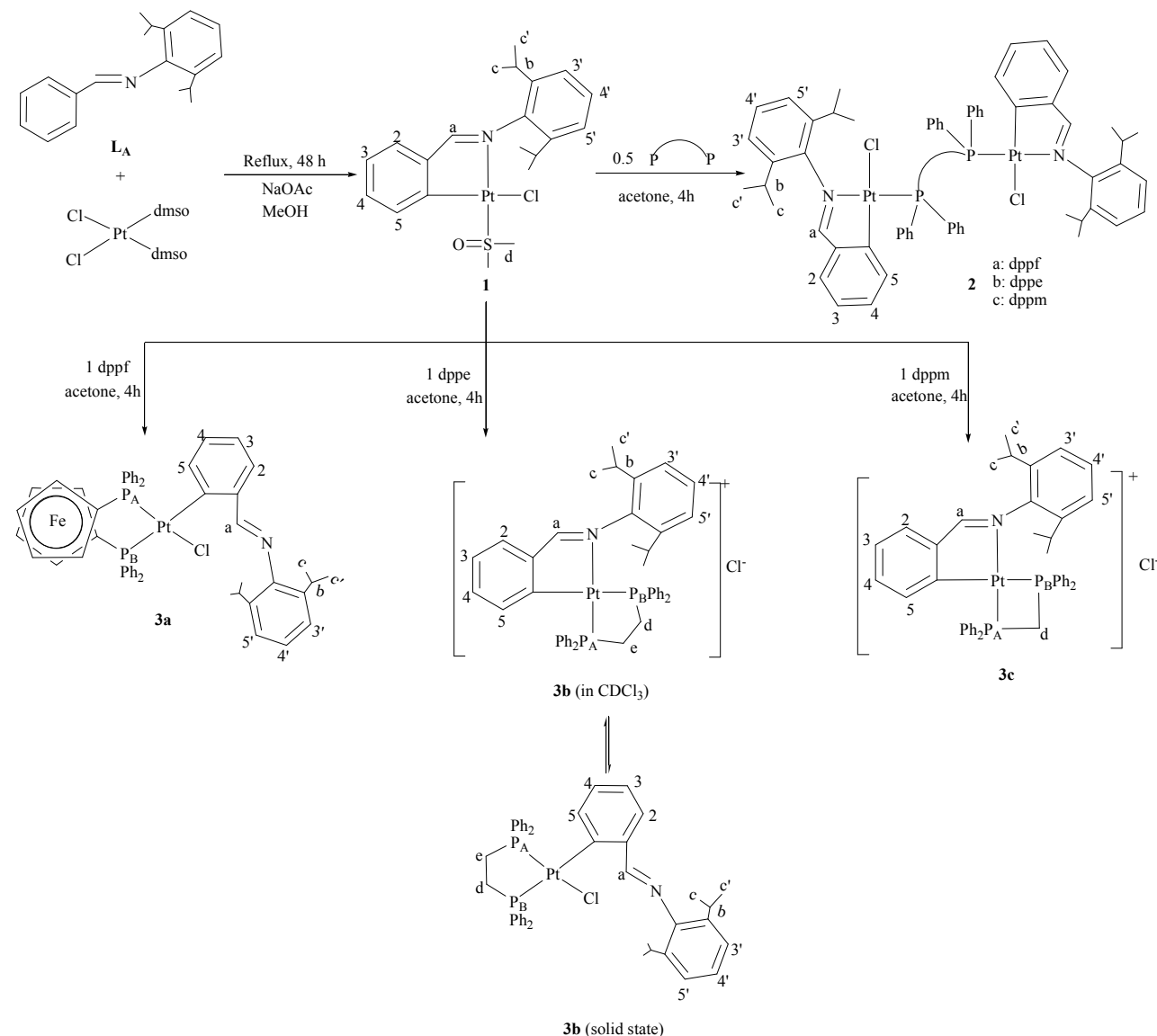
2.1. Synthesis of the complexes

The routes to prepare the cyclometallated Pt complexes are described in Scheme 1. The reaction of *cis*-[PtCl₂(dmsO)₂] with 1 equivalent of benzylidene-2,6-diisopropylphenylamine (**L_A**) in the presence of sodium acetate, in refluxing methanol gave complex [PtCl(N[^]C)(dmsO)], **1**. The reactions of **1** with 0.5 mole equivalent of a bidentate phosphine ligand (biphos) such as dppf (a), dppe (b) and dpmm (c) at room temperature in acetone, gave

Cite this: DOI: 10.1039/c0xx00000x

www.rsc.org/xxxxxx

ARTICLE TYPE



Scheme 1 The mononuclear and binuclear cyclometallated platinum(II) complexes containing bidentate phosphines

in good yield the binuclear complexes of the type $[\text{Pt}_2\text{Cl}_2(\text{N}^{\wedge}\text{C})_2(\mu\text{-P}^{\wedge}\text{P})]$, **2a-2b**, by replacement of the dmsO ligands with the P donor atoms of the diphosphine.

In the reaction of $[\text{PtCl}(\text{N}^{\wedge}\text{C})(\text{dmsO})]$ with 1 equivalent of dppf, which has the largest bite angle amongst the three diphosphines studied, the cleavage of the Pt-N bond is observed resulting in the formation of the monodentate complex $[\text{PtCl}(\text{dppf})(\text{N}^{\wedge}\text{C}-\kappa^1\text{C})]$, **3a**. The reaction with dppm which has the smallest bite angle, produces a rather unstable ionic complex **3c**, in which both the imine and the bisphosphine behave as bidentate ligands. It is noteworthy that the reaction of **1** with dppe leads to formation complex **3b**, which shows an unusual intramolecular

transformation between the neutral monodentate $[\text{N}^{\wedge}\text{C}-\kappa^1\text{C}]$ and ionic bidentate $[\text{N}^{\wedge}\text{C}]$ system. The ^1H NMR spectrum of **3b** recorded in CDCl_3 , as well as its solution IR spectrum recorded in DCM, indicated the presence of the ionic species with the bidentate $[\text{N}^{\wedge}\text{C}]$ ligand in solution. On the contrary, the IR spectrum of the compound recorded as a KBr pellet and the X-ray crystal structure of **3b** confirmed a neutral species in the solid state in which the imine nitrogen is not coordinated to the platinum centre.

2.2. Characterization of the complexes

The ^1H NMR data for the cyclometallated complex **1** agrees with

the data reported for similar complexes.^{3a} By replacing the dmsu group with the diphosphines, all the imine proton (H^b) signals of the complexes, except that of **3a**, were significantly shifted downfield to the region δ 8.13 – 8.28 ppm, and appeared as a doublet as a result of coupling to platinum. The imine proton for **3a**, however, appeared as a singlet at δ 9.16 ppm, indicating that the imine N is not coordinated to the metal.

In the 1H NMR spectrum of each binuclear complex, three well-separated peaks with a relative intensity of 1:1:1 were observed in the aromatic region. This included the downfield doublet of triplets for H^3 and H^4 protons, and a more upfield signal for the H^5 proton. The up-field chemical shift of H^5 relative to the analogous signal in **1** has been ascribed to the anisotropic shielding effect of the aromatic ring in diphosphine ligands.^{2a} The two isopropyl groups are non-equivalent in all the dinuclear complexes, and appeared as two doublets. In contrast to the dinuclear analogues, the 1H NMR spectra of the mononuclear complexes **3** show overlapping of signals in the aromatic region. Two broad singlets were also observed for the isopropyl methyl groups in the spectra of the dppe and dppm complexes **3b** and **3c**, which are resolved into two doublets at low temperature due to the fluxional motion of the aromatic ring containing the isopropyl units.

In the ^{13}C -NMR spectra for the dinuclear complexes, the imine carbon (C^a) and the aromatic carbon adjacent to the metallation site (C^5) appear as doublets and are coupled to platinum (J_{Pt-C^5} ca. 80 – 85 Hz and J_{Pt-C^a} ca. 85 – 92 Hz, respectively). However, the resonance of the imine carbon in the dppe and dppm chelated mononuclear complexes **3b** and **3c**, exhibit an upfield singlet at 184.92 and 183.86 ppm, respectively, compared to the dinuclear complexes for which the analogous signal appears at ca. 179 ppm. The imine carbon of the dppf chelated complex **3a**, showed a significant downfield singlet at 166.34 ppm, corresponding with the resonance of the imine signal of the free N^C ligand, indicating that in this case the imine N is not coordinated to the metal.

In ^{31}P NMR spectra of the binuclear complexes, $[Pt_2Cl_2(N^C)_2(\mu-P^A P^B)]$, **2**, the two equivalent P atoms appeared as a sharp singlet for each of the analogues. The equivalence of the P atoms suggests that the diphosphine ligands act as a spacer between the two $Pt(N^C)$ moieties, and each P atom is coordinated to a Pt atom in a trans position to the N atom of the N^C ligand. Virtual coupling was also observed for complexes **2b** and **2c**. On the contrary, the ^{31}P NMR spectra of mononuclear complexes **3**, show two sets of resonances due to non-equivalent phosphorous atoms, both coupled to platinum. The higher J value is assigned to the phosphorus atom *trans* to the chloride ligand (for **3a**) or imine nitrogen (for **3b** and **3c**) and the lower to that *trans* to the metallated carbon, which is in agreement with the reported values for related complexes.^{2a,4b,8} The different $^1J_{Pt-P}$ values for the chelating complexes are due to the *trans* influence of the metallated C atom being much greater than that of the chloride ligand or the imine nitrogen. A case in point is the complex **3a** where the $Pt-P_A$ bond length, i.e. *trans* to chloride, is approximately 0.15 Å (*vide infra*) shorter compared with the $Pt-P_B$ bond. Furthermore, the ^{31}P NMR spectrum of complex **3a** exhibit considerable 2nd order or strong coupling effects illustrated in Figure 1a at 313 K, i.e. characteristic “roofing” of

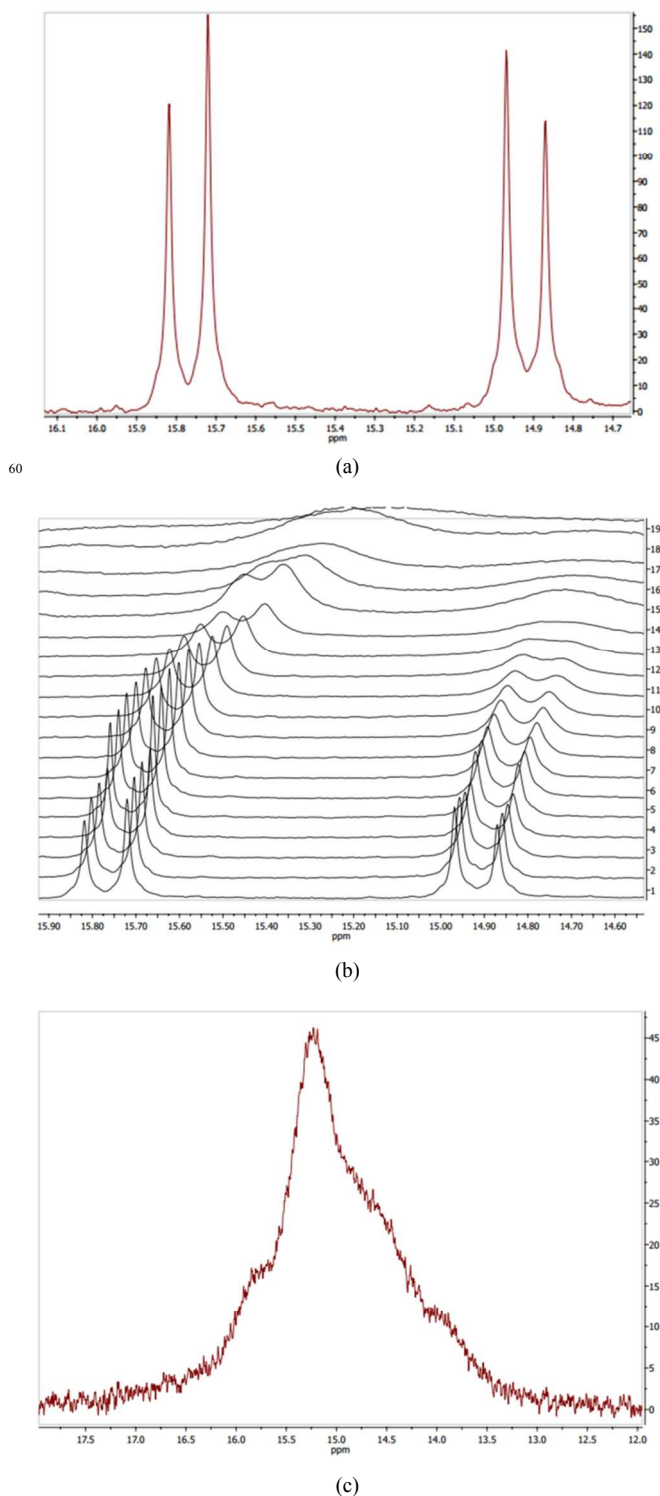


Fig. 1 (a) ^{31}P NMR spectrum of complex **3a**; (b) variable temperature ^{31}P NMR spectrum of complex **3a**; (c) ^{31}P NMR spectrum at 223 K

the doublets at 14.89 and 15.74 ppm respectively, with an estimated $\Delta\nu/J$ ratio of 6.43 consistent with an AB spin system. As temperature is decreased from 313 to 223 K the ^{31}P NMR resonances at 14.89 and 15.74 ppm broaden significantly and both shift upfield, Figure 1b, whilst the $\Delta\nu/J$ ratio continually decrease yielding stronger 2nd order coupling effects. At 223 K it seems that these resonances are relatively close to coalescence,

Figure 1c, suggestive of a dynamic site exchange reaction. However, in a relatively recent communication by James and co-workers^{[1]9} it is shown how a set of Ru(II) diphosphine/diimine complexes exhibit remarkable ³¹P NMR temperature dependent spectra in which the expected AB pattern is sometimes 'lost' as a function of decreasing temperature giving rise to accidental degeneracy or an A₂ pattern. Upon a further temperature decrease the A₂ resonance pattern converts back to the expected AB. It is also clear that these ³¹P NMR temperature dependent spectra are not due to dynamic exchange processes between 2 or more conformers/species yielding time averaged resonance patterns. Furthermore, James^{[1]9} also found that the temperature where A₂ patterns occur instead of AB or AX varies as a function of solvent and ligand type *trans* to the coordinating phosphor donor atoms.

In a variable temperature ³¹P NMR study conducted by Lynam and co-workers^{[2]10}, it was observed that the AB resonance pattern at 300 K for complex [Ru(E-Ch=C{PPh₃}R(η⁵-C₅H₅)(PPh₃)₂][OTf], varies considerably with temperature and at 240 K an A₂ pattern is obtained. At still lower temperatures the AB resonance pattern re-emerges. Simulations performed by Lynam^{[2]10} showed that the changes in lineshape of these resonances can be accounted for by changes in chemical shift as a function of temperature rather than dynamic exchange processes. The relatively large changes in chemical shift and lineshape pattern for complex 3a (AB resonance pattern tending to an A₂ pattern, Figures 9 a-c) as a function of decreasing temperature emulates the data of James^{[1]1} and Lyman^{[2]1}. Moreover, taking into account that the only other stable conformer as found via DFT calculations is 10 kCal.mol⁻¹ higher in energy (*vide infra*) leads us to the conclusion that dynamic exchange processes is not responsible for the line shape changes shown in Figure 9b but rather temperature induced chemical shifts in the presence of 2nd order coupling effects. We are currently investigating this phenomenon further given the importance of ³¹P NMR as a characterization method for organometallic compounds.

It is interesting to note that the ν_{C=N} stretching vibration for **3b** with dppe ligand is at 1601 cm⁻¹ when recorded in CH₂Cl₂ solution, while at 1631 cm⁻¹ when recorded as a KBr pellet (see Figure S1). This indicates the Pt-N bond in **3b** forms in CH₂Cl₂ solution and cleaves in the solid state. Similar intraconversion behaviour was not observed for either **3a** or **3c**. NMR and IR spectroscopic data for the dppf complex **3a** is consistent with the neutral species monodentate [N[^]C-κ¹C] ligand in both the solid state and in CH₂Cl₂ solution, while the dppm analogue **3c** remains as a cationic species with bidentate [N[^]C] ligand in both the solid phase and in solution.

To further confirm the nature of the mononuclear complexes, their conductivities were determined in CH₂Cl₂ at 25 °C. 1 mM solutions were used to measure conductivities. The cationic character of the complexes containing dppe and dppm, **3b** and **3c**, was confirmed by the relatively larger molar conductivities, 58.0 and 66.1 Ω⁻¹.cm².mol⁻¹, respectively. These Λ_M values indicated that both dppe and dppm complexes were 1:1 electrolytes. On the contrary, the dppf complex **3a**, shows neutral character as determined by ¹H NMR and IR spectroscopies, and showed very low molar conductivity in CH₂Cl₂ (see Table S1). This is similar to what is observed for that of the neutral dinuclear complex, **2c**.

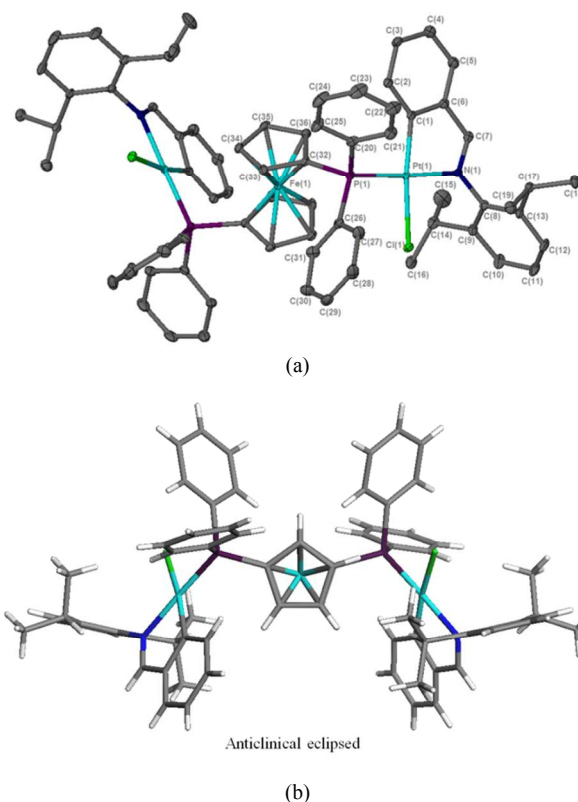


Fig. 2 (a) Molecular structure of **2a** showing the atomic numbering scheme. All H atoms are omitted for clarity. All non-hydrogen atoms are presented as an ellipsoidal model with probability level 30%. (b) Conformation of the cyclopentadienyl rings of the ferrocene moiety in complex **2a**.

2.3. Crystal structures

Suitable crystals were grown from dichloromethane/methanol (**2c**), and dichloromethane/n-hexane (**3a**) at low temperature (*ca.* 4 °C), or by slowly evaporating dichloromethane/n-hexane (**2a**), and acetone (**3b**) solutions of the complexes. The labeling schemes for all the compounds are shown in Figures 2 – 4. Selected interatomic distances and angles are listed in Table 1.

All the molecular structures exhibit distortions from idealized square-planar geometry at the metal. Complexes **3a** and **3b** are mononuclear species with the diphosphine acting as a chelating ligand. In contrast, complexes **2a** and **2c** have a crystallographic two-fold symmetry and sits astride a two-fold axis, making only one-half of the complex unique. Two planes containing a Pt atom are connected via the diphosphine ligand. The P atom occupies the *trans* position to the N atom in both **2a** and **2c**.

The platinum atoms in complexes **3a** and **3b** are surrounded by a chelating dppf or dppe ligand, C and Cl atoms. This reveals that the strong chelating ability of the diphosphine ligands has caused the Pt-N bond of the cyclometallated complex to undergo cleavage, forming the neutral complexes with a monodentate η¹-C-bond to the platinum centre in the solid state.

For the dppf containing complexes, the mutual arrangement of the two Cp rings is measured by the Cp(centroid)-Fe-Cp(centroid) twist angle(τ)

and the dihedral angle between the mean planes through the Cp rings (θ) (see Table S2). For the dinuclear complex **2a**, the Cp(centroid)-Fe-Cp(centroid) twist angle is 143.5°, so the dppf is

Cite this: DOI: 10.1039/c0xx00000x

www.rsc.org/xxxxxx

ARTICLE TYPE

Table 1 Selected bond lengths (Å), bond angles (°) and torsion angles (°) for complexes **2a**, **2c**, **3a** and **3b**

2a		2c		3a		3b	
Pt(1)–C(1)	2.005(9)	Pt(1)–C(1)	2.016(4)	Pt(1)–C(1)	2.048(6)	Pt(1)–C(1)	2.073(3)
Pt(1)–N(1)	2.077(8)	Pt(1)–N(1)	2.085(4)	Pt(1)–P(1)	2.2308(15)	Pt(1)–P(1)	2.2193(7)
Pt(1)–P(1)	2.231(2)	Pt(1)–P(1)	2.2370(10)	Pt(1)–P(2)	2.3517(17)	Pt(1)–P(2)	2.3120(7)
Pt(1)–Cl(1)	2.364(2)	Pt(1)–Cl(1)	2.3654(10)	Pt(1)–Cl(1)	2.3507(16)	Pt(1)–Cl(1)	2.3592(6)
N(1)–C(7)	1.287(13)	N(1)–C(7)	1.283(5)	N(1)–C(7)	1.267(9)	N(1)–C(7)	1.271(4)
C(1)–Pt(1)–N(1)	80.3(3)	C(1)–Pt(1)–N(1)	80.60(14)	C(1)–Pt(1)–Cl(1)	86.26(16)	C(1)–Pt(1)–Cl(1)	89.09(7)
C(1)–Pt(1)–P(1)	97.2(3)	C(1)–Pt(1)–P(1)	97.13(11)	C(1)–Pt(1)–P(1)	87.87(16)	C(1)–Pt(1)–P(1)	91.78(7)
N(1)–Pt(1)–Cl(1)	90.7(2)	N(1)–Pt(1)–Cl(1)	89.23(9)	P(2)–Pt(1)–Cl(1)	86.27(5)	P(2)–Pt(1)–Cl(1)	92.20(2)
P(1)–Pt(1)–Cl(1)	91.87(8)	P(1)–Pt(1)–Cl(1)	92.55(4)	P(1)–Pt(1)–P(2)	99.50(5)	P(1)–Pt(1)–P(2)	86.88(3)
Total 1 ^a	360.2	Total 1 ⁱ	359.5	Total 1 ^a	359.9	Total 1 ^a	360.0
C(1)–Pt(1)–N(1)	80.3(3)	C(1)–Pt(1)–N(1)	80.60(14)			P(1)–Pt(1)–P(2)	86.88(3)
C(7)–N(1)–Pt(1)	114.4(6)	C(7)–N(1)–Pt(1)	113.7(3)			C(33)–P(2)–Pt(1)	105.32(10)
C(6)–C(1)–Pt(1)	113.3(6)	C(6)–C(1)–Pt(1)	112.2(3)			C(32)–P(1)–Pt(1)	108.25(9)
C(1)–C(6)–C(7)	114.0(9)	C(1)–C(6)–C(7)	115.8(3)			C(33)–C(32)–P(2)	110.16(19)
N(1)–C(7)–C(6)	118.0(9)	N(1)–C(7)–C(6)	117.7(3)			C(33)–C(32)–P(2)	109.69(19)
Total 2 ^b	540.3	Total 2 ⁱⁱ	540.1			Total 2 ^b	520.3
N(1)–Pt(1)–C(1)–C(2)	-178.6(9)	N(1)–Pt(1)–C(1)–C(2)	-174.1(4)				
Pt(1)–N(1)–C(8)–C(13)	-95.4(10)	Pt(1)–N(1)–C(8)–C(13)	-87.5(4)				

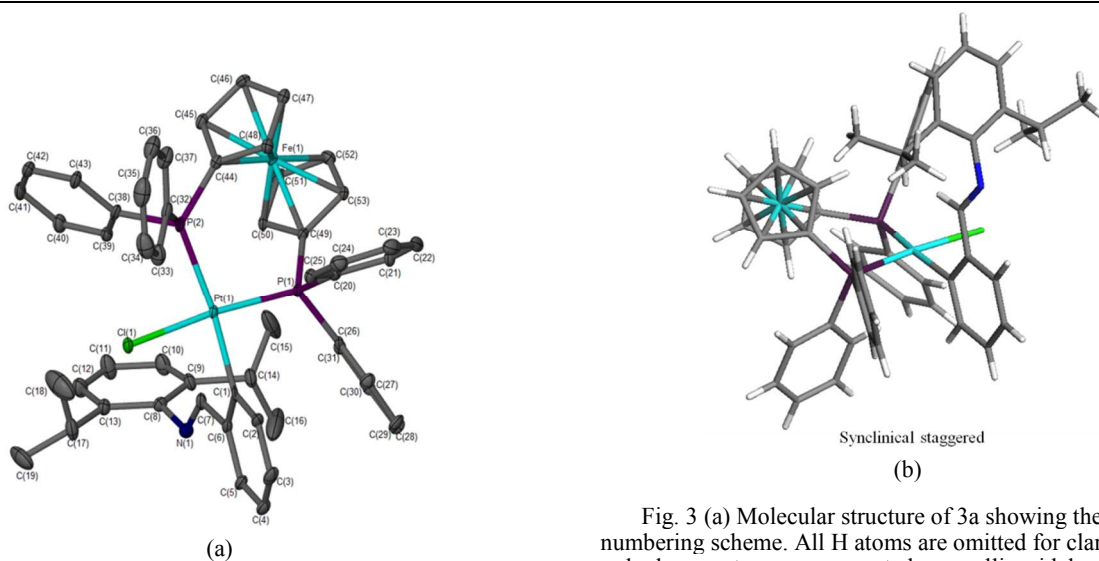
^a Sum of angles in the coordination environment of the platinum atom. ^b Sum of internal angles of the metal-containing ring.

Fig. 3 (a) Molecular structure of **3a** showing the atomic numbering scheme. All H atoms are omitted for clarity. All non-hydrogen atoms are presented as an ellipsoidal model with probability level 30%. (b) Conformation of the cyclopentadienyl rings of the ferrocene moiety in complex **3a**.

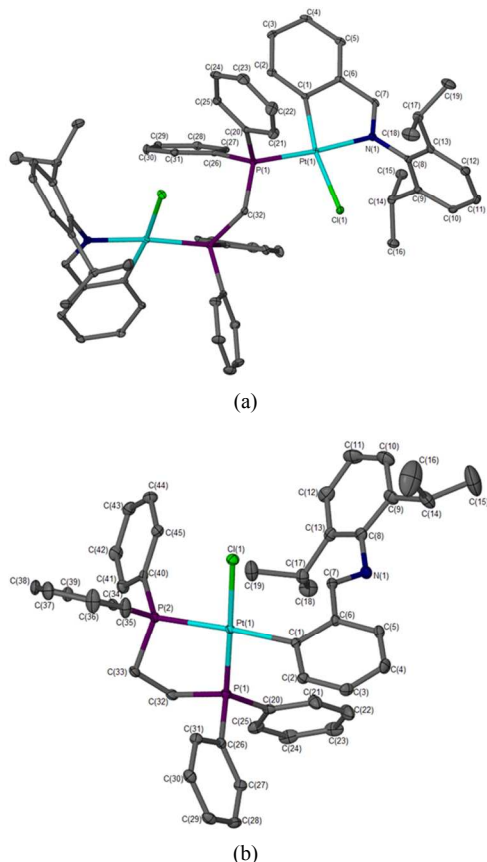
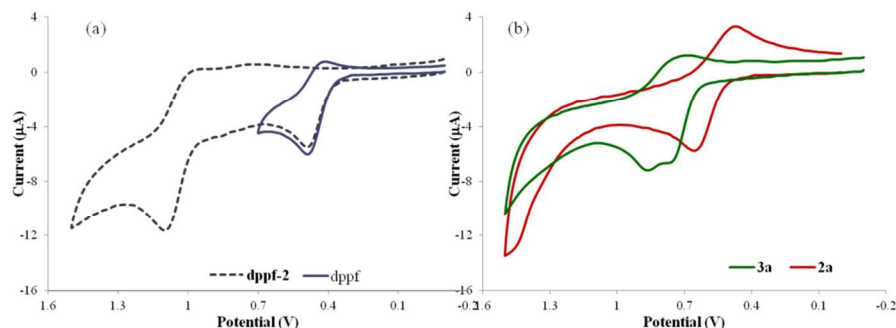


Fig. 4 Molecular structure of (a) **2c** and (b) **3b** showing the atomic numbering scheme. All H atoms are omitted for clarity. All non-hydrogen atoms are presented as an ellipsoidal model with a probability level of 30%. The solvent molecule has been omitted in this diagram.

arranged in a nearly ideal “anticlinal eclipsed” conformation. This is in agreement with related dinuclear platinum^{4b} and palladium¹² complexes. In the structure of **3a**, the dppf ligand adopts a “synclinal staggered” arrangement⁹ which is defined by the Cp(centroid)-Fe-Cp(centroid) twist angle of 39.2°.

2.4. Electrochemical and Photochemical Properties

Redox properties of the dppf complexes. The main interest in the use of dppf as a ligand stems from the unusual bite angle of the chelating phosphine together with the presence of the redox-active ferrocene backbone. The cyclic voltammograms of freshly prepared solutions (1.5 mM) of dppf, the dinuclear complex **2a**

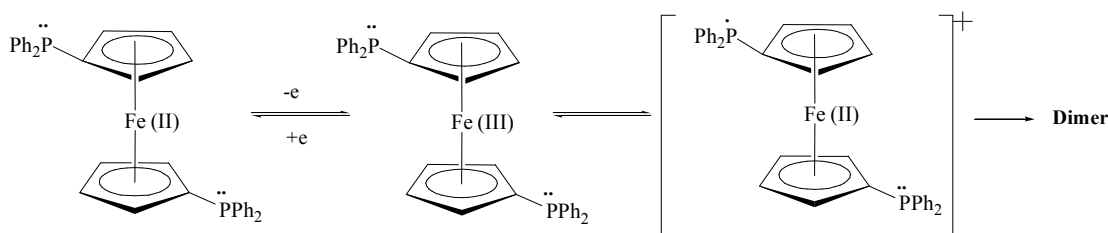


and mononuclear complex **3a** in dichloromethane were recorded at 298 K. These are presented in Figure 5.

Numerous studies have investigated the oxidative electrochemistry of dppf, which, unlike that of simple ferrocene, is complicated by a side reaction that has been proposed to involve a dimerization process (Scheme 3).^{13(a)} This dimerization often impacts on the nature of the CV plot obtained for dppf containing compounds. As shown in Figure 5 (a), in the narrow scan range (< 0.7 V), the dppf ligand exhibits a single, reversible oxidation wave at $E_{1/2} = 0.460$ V due to the oxidation of the ferrocene moiety, which agree with the reported value (0.450 V).^{13(b)} In the wider scan range (up to 1.6 V), the secondary reaction which occurs can be detected and is based on the oxidation of the phosphine group at $E_{1/2} = 1.04$ V ($E_{pa}^2 = 1.10$ V). The irreversible oxidation process of the ferrocene moiety could be attributed to a dimerization process.

The platinum complexes **2a** and **3b** show different redox behaviour in CH_2Cl_2 depending on the coordination mode of dppf (Figure 5b). Both complexes show greater anodic half-wave potentials compared to the uncoordinated dppf ligand due to the electron-withdrawing property of the ligand and the Lewis acidic character of the Pt(II) ion. The dinuclear complex, **2a**, exhibits only one reversible redox peak at $E_{1/2} = 0.567$ V ($E_{pa} = 0.654$ V, $E_{pc} = 0.480$ V), and it has the more cathodic potential of two complexes. It suggests that Fc^+ formed during the oxidation process is well stabilized by the $[\text{Pt}(\text{N}^{\wedge}\text{C})]$ moiety, and no oxidation occurs on phosphine groups. On the other hand, the cyclic voltammetry of the mononuclear complex, **3a**, suggests multi-electron transfer. The forward peaks show overlapping of two oxidation processes, while the reverse peak displays a much broader shape, which could be due to two unresolved reductive process. The first redox peak at $E_{pa}^1 = 0.765$ V ($E_{1/2}^1 = 0.738$ V) can be assigned to the redox process related to the ferrocene moiety. The second redox peak at $E_{pa}^2 = 0.785$ V ($E_{1/2}^2 = 0.748$ V) corresponds to the redox processes of the phosphine group, a subsequent dimerization reaction that has been proposed for dppf.¹³ The half-wave potential of the oxidation process of phosphine groups is much more cathodic compared to that of free dppf which occurs at $E_{1/2} = 1.04$ V (see Fig. 5a and Table S4), indicating that the chelating coordination mode where two phosphine atoms bound to the same Pt centre, thus increasing the electron density on the metal making this oxidation much more feasible. Consequently, the oxidation of the ferrocene moiety is more different.

Fig.5 Cyclic voltammograms scan of the oxidation of 1.5 mM dppf (a), **2a** and **3a** (b) in CH₂Cl₂/0.10 M TBAP at 100 mV/s.



Scheme 2. Proposed dimerization reaction of dppf^{13(a)}

5

Absorption spectra. The UV-Vis absorption spectra of the complexes were recorded in CH₂Cl₂ at 298K for all the cyclometallated Pt complexes (see Figure S3 and Table S5). All the complexes give rise to intense absorptions between 235 and 340 nm, which match the absorption range observed for free C[^]N ligand,¹⁴ and thus assignable to metal-perturbed ligand-centred transitions (¹LC $\pi-\pi^*$). The low-energy transitions in the range of 370 – 450 nm, with extinction coefficients between 2000 and 6000 M⁻¹cm⁻¹ were previously assigned as metal-to-ligand charge transfer (¹MLCT) for most C[^]N-cyclometallated Pt(II) complexes.^{1,15} In the visible region of the absorption spectra of complexes **1** and **2a-c**, there is a broad charge-transfer maximum at ca. 410 nm with a slight shoulder ca. 430 nm. In view of their significant extinction coefficients, the corresponding electronic states are assigned as ¹MLCT. Changing of the bridging phosphine ligand (dppf, dppe or dppm) has hardly any effect on the lower-energy absorption bands of the dinuclear complexes. In contrast to the dinuclear analogues, no absorptions between 370 – 450 nm assigned to ¹MLCT were observed in the mononuclear complexes **3a-c**, due to the fact that the HOMO and LUMO are largely located on the C[^]N moiety with no or very little contribution from Pt the centre.¹

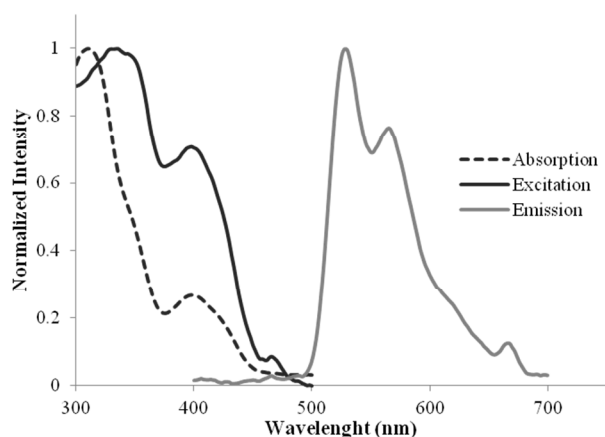


Fig.6 Excitation, emission and absorption spectra of complex **1** in CH₂Cl₂ (10⁻⁴ M) at 298 K.

30

Excitation and Emission spectra. The dppe and dppm complexes as well as the dmsO precursor are emissive in a CH₂Cl₂ solution at 298 K. The excitation and emission data are

summarized in Table S6. The emission spectra of **1** in CH₂Cl₂ at 298 K show an incipient vibronic structure (Figure 6). The corresponding excitation spectra match the room-temperature absorption spectrum. By replacing the dmsO group with the phosphine ligands, the excitation spectra of all complexes lose the features observed in the spectrum of **1** and give structureless excitation bands (Figure 7). For the dinuclear complexes **2b** and **2c**, the excitation spectra show low-energy bands, while high-energy bands are observed for mononuclear complexes. This agrees with the observation where low energy bands are absent in the UV-Vis spectra of the mononuclear complexes.

In all the cases, the emission spectra (Figure 8) reveal vibronic structures. Both dinuclear complexes give rise to somewhat structured emission at 532 nm (max), similar to that of **1**. Significant blue shifts relative to the emissions of the dinuclear complexes are observed for the mononuclear analogues, especially for the dppe complex **3b**. This could also be attributed to the absence of ¹MLCT in the mononuclear complexes.

2.5. Computational study

Due to the unusual behaviour of the complexes, **3b** and **3c**, we decided to investigate these computationally. An overall agreement has been found between the calculated and experimental structures of the neutral conformer for the dppe complex **3b**. According to the theoretical results (Figure 9), the neutral isomer **3bN** was found to be the species with the lowest energy, whereas the cationic isomer **3bC** was found to be 7.2 kcal/mol higher in energy. Dppm has the smallest bite angle among the three diphosphines and in the case of its analogue **3c** (Figure 10), the two conformers have very close energies, with the cationic isomer **3cC** being found to be 4.4 kcal/mol higher than its neutral isomer **3cN**. The differences in energy between the neutral and cationic conformers of **3b** and **3c** can be employed to rationalize the experimental findings. Thus in the case of the dppm complex, **3c** the computational studies show small energy difference between the neutral and cationic conformers, and in reality we observe only the cationic conformer both in the solid state as well as in solution (CH₂Cl₂ and CH₃Cl). For the dppe system theoretical calculations show a larger energy difference between the neutral and cationic conformers. In this instance the neutral isomer was experimentally isolated in the solid state while the cationic isomer was detected in solution for the dppe complex **3b**.

70

75

Cite this: DOI: 10.1039/c0xx00000x

www.rsc.org/xxxxxx

ARTICLE TYPE

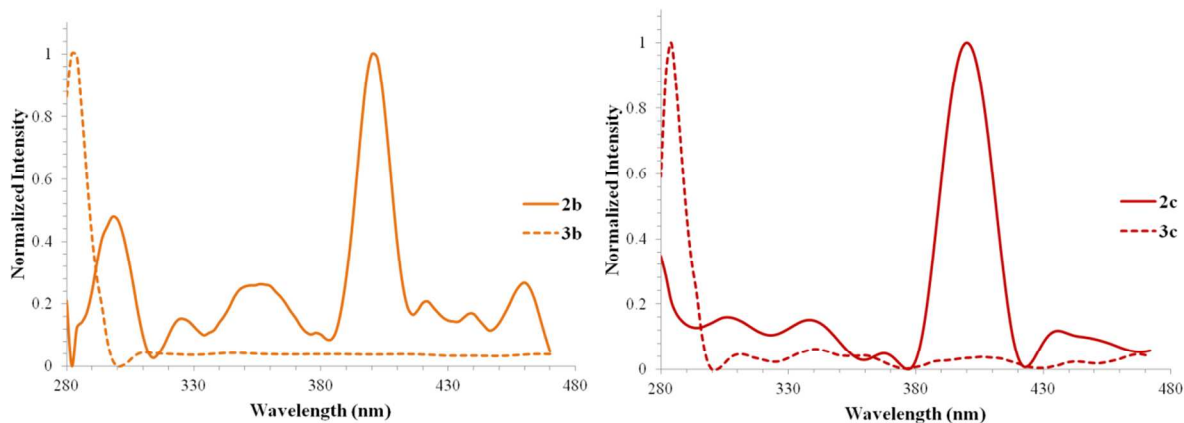


Fig. 7 Caption Excitation spectra of the cyclometallated Pt complexes **2b-c** and **3b-c** in CH_2Cl_2 (10^{-4} M) at 298 K.

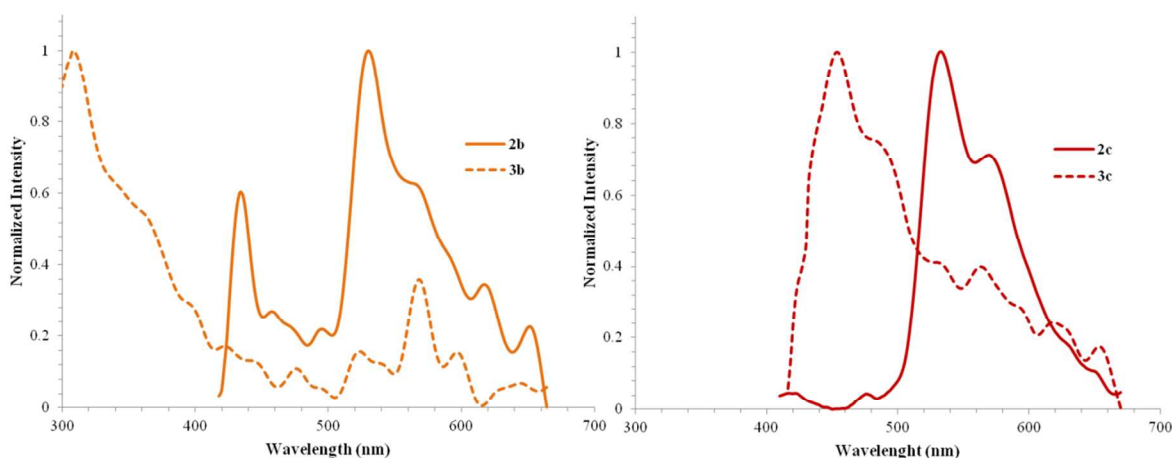


Fig. 8 Emission spectra of the cyclometallated Pt complexes **2b-c** and **3b-c** in CH_2Cl_2 (10^{-4} M) at 298K.

Attempts, to optimize the molecular structure of cationic conformer of the dppf complex **3a**, did not give the expected structure (Figure 11). The calculated structure (**3aN-2**) is neutral with the Cl still bonded to the Pt centre, and with the Pt-N distance being 3.202 Å. The molecular structure of the neutral conformer (**3aN-1**) was optimized based on the X-ray structure, with the Pt-N distance being 4.622 Å. The energy difference between these two structures is found to be 3.4 kcal/mol in favour of **3aN-1**. The unsuccessful optimization of the cationic isomer of **3c** could possibly be attributed to the larger bite angle of dppf. This points to instability of the cationic species and is consistent with the experimental observation where **3c** remains as the neutral conformer in both the solid state and in solution.

3. CONCLUSIONS

The reactions of diphosphines with the dmsoligated cyclometallated platinum compound **1** have been studied in the present work. When diphosphines were used as spacer ligands (in a molar ratio of 2:1 to Pt), dinuclear complexes **2a – 2c** were obtained, while in an equimolar ratio, the P[^]P chelated mononuclear complexes **3a – 3c** were isolated.

In the mononuclear derivatives, the cleavage of the Pt-N bond of the platinumacycles depends on the bite angle of the diphosphine ligands. For compound **3b** containing dppe, which has a medium bite angle compared to the other diphosphines studied, dppe

caused cleavage of the Pt-N bond of the metallacycle leading to a monodentate [N-C- κ^1 C] system in the solid state, and with extrusion of the chloride ligand giving an ionic derivative in CDCl₃ or DCM. A fluxional behaviour was observed for compound **3b** and **3c** in solution, both of which are ionic in nature in solution.

A comparative study of structures, electrochemical and photochemical properties between both dinuclear and mononuclear complexes was also reported and found these properties are largely depending on the nature and the coordination mode of the diphosphines.

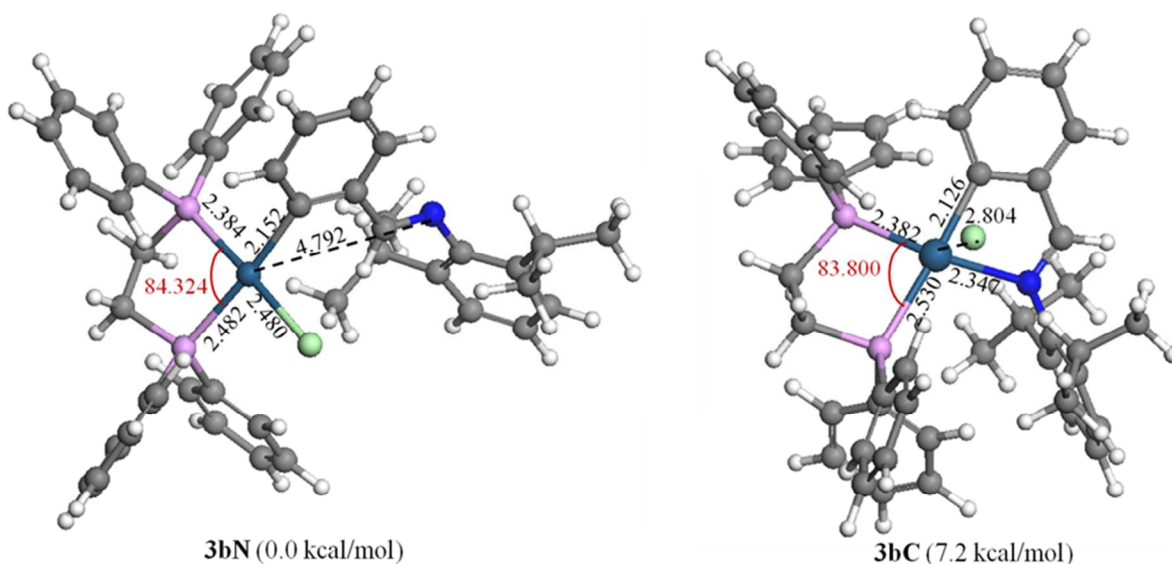


Fig. 9 Optimized structures of **3b** in both neutral and cationic forms. Calculated Gibbs free energies ($\Delta G_{298.15K}$) at 298.15 K, 1 atm and in chloroform in kcal/mol relative to **3bN** are given in brackets. Note: the bite angles of the diphosphine ligands are given in red.

15

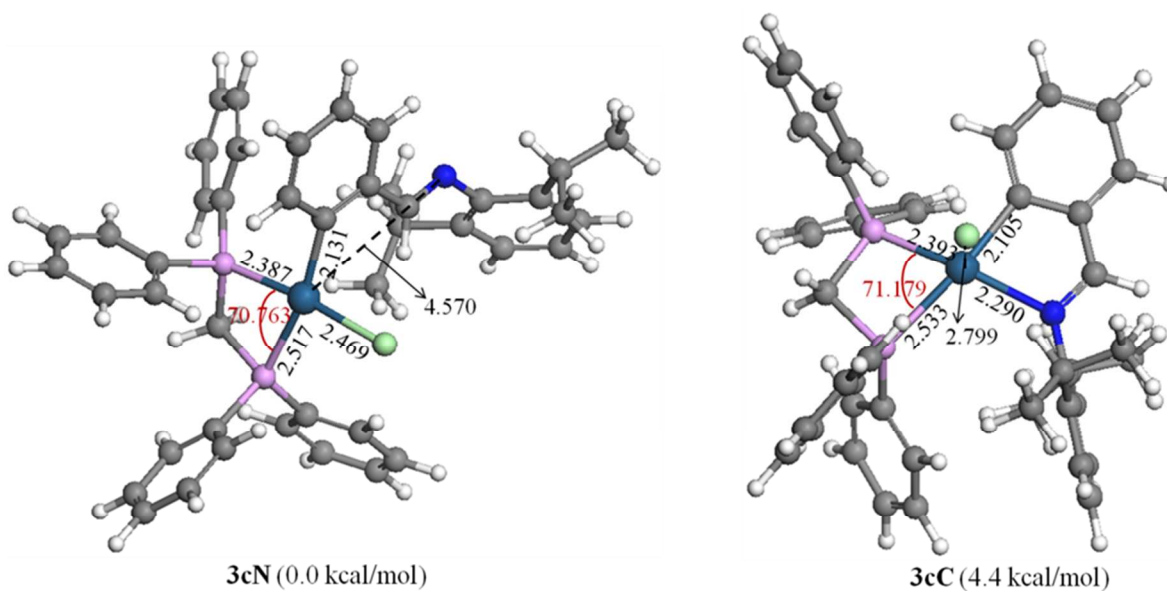


Fig. 10 Optimized structures of **3c** in both neutral and cationic forms. Calculated Gibbs free energies ($\Delta G_{298.15K}$) at 298.15 K, 1 atm and in chloroform in kcal/mol relative to **3cN** are given in brackets. Note: the bite angles of the diphosphine ligands are given in red.

20

Cite this: DOI: 10.1039/c0xx00000x

www.rsc.org/xxxxxx

ARTICLE TYPE

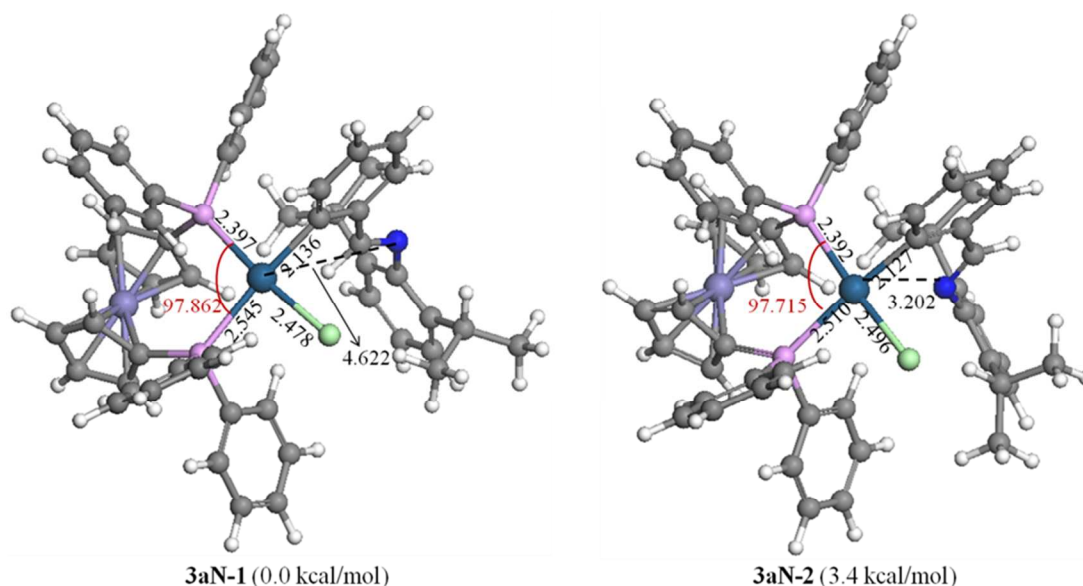


Fig. 11 Optimized structures of **3a**. Calculated Gibbs free energies ($\Delta G_{298.15K}$) at 298.15 K, 1 atm and in chloroform in kcal/mol relative to **3aN-1** are given in brackets. Note: the bite angles of the diphosphine ligands are given in red.

4. Experimental Section

4.1. General

The solvents were purified and distilled by standard methods. Methanol (dry, max. 0.005% H₂O) was purchased from Aldrich.

NMR spectra were recorded on a Varian Mercury-300 MHz or Varian Unity-400 MHz spectrometer. Residual solvent signals were used as a reference when recording ¹H and ¹³C NMR spectra. H₃PO₄ (85% in D₂O) were used for reference as ³¹P NMR. Abbreviations used: s = singlet, d = doublet, t = triplet, m = multiplet, b = broad, NMR labelling as shown in Scheme 1. Infrared spectra were recorded as KBr disks and measured on a Perkin Elmer Spectrum One FT-IR spectrophotometer. Mass spectral analyses were carried out at Stellenbosch University on a Waters Q-TOF Ultima API or Waters Quattro Micro API mass spectrometer using the electrospray ionization technique. Elemental analyses were carried out on a Fisons EA 1108 CHNS Elemental Analyzer at the microanalytical laboratory of the University of Cape Town. Melting points were recorded on a Kofler hotstage microscope (Reichert Thermovar). Conductivity in dichloromethane (1 mM concentration) was measured using a Crison Basic 30+ Conductivity meter. UV-vis spectra (Figure S4), excitation spectra (Figures 6-7) and emission spectra (Figure 8) were obtained using a Chirascan / Chirascan-plus CD Spectrometer

Cyclic voltammetry was performed at ambient temperature by

using a Bioanalytical Systems Inc. BAS 100W Electrochemical Analyser with a one-compartment three-electrode cell comprising a platinum disk working electrode, a platinum wire auxiliary electrode and a Ag/Ag⁺ reference electrode (0.01 M AgNO₃ and 0.1 M [n-Bu₄N][ClO₄] in anhydrous acetonitrile). The reported E values (see text and Table S4) are with reference to this electrode. Measurements were made on anhydrous acetonitrile solutions that were ca. 1.5 mM in sample and contained 0.1 M [n-Bu₄N][ClO₄] as background electrolyte. A scan rate of 100 mV s⁻¹ was used throughout, with scans starting from the most negative potential and initially scanning anodically. Under these conditions the half-wave potential of the ferrocene/ferrocenium couple, which was used as a reference, never varied by more than 0.03 V from a mean value of $E_{1/2} = +0.18$ V vs. the Ag/Ag⁺ reference electrode, and had a peak separation falling between $\Delta E_p = 59$ and 66 mV. All solutions were purged with argon and voltammograms were recorded under a blanket of argon. The platinum disk working electrode was polished between runs.

X-ray single crystal intensity data for all structures were collected on a Bruker KAPPA APEX II DUO diffractometers using graphite monochromated MoK α radiation ($\lambda = 0.71073$ Å). Temperature was controlled by an Oxford Cryostream cooling system (Oxford Cryostat). The strategy for the data collections was evaluated using the Bruker Nonius "Collect" program. Data were scaled and reduced using DENZO-SMN software.¹⁶ An empirical absorption correction using the program SADABS¹⁷ was applied. The structure was solved by direct methods and refined employing full-matrix least-squares with the program

SHELXL-97¹⁸ refining on F². Packing diagrams were produced using the program PovRay and the graphic interface X-seed.¹⁹ All the non-hydrogen atoms were refined anisotropically. The hydrogen atoms were placed in idealised positions in a riding model with U_{iso} set at 1.2 or 1.5 times those of their parent atoms and fixed C-H bond lengths.

4.2. Preparation of the compounds

1 was obtained from *cis*-[PtCl₂(SOMe₂)₂] (0.556 g, 1.32 mmol), imine ligand **L_A**, (0.0350 g, 1.32 mmol) and sodium acetate (0.210 g, 2.65 mmol), which were allowed to react in dry methanol at 65 °C for 48 h. The reaction mixture was filtered through celite to remove metallic platinum. The solvent was removed on a rotary evaporator and the residue was recrystallized using dichloromethane-methanol, yielding a deep yellow crystalline solid which was isolated by filtration in *vacuo*. Yield 0.218 g (29%). m.p.: 194 – 196 °C. IR (KBr): ν (CH=N) 1601 cm⁻¹, (S=O) 1139 cm⁻¹. ¹H NMR (400 MHz, CDCl₃): δ = 8.31 [d, ⁴J_{H-H} = 7.83 Hz, ³J_{Pt-H} = 40.1, 1H, H⁵], 7.95 [s, ³J_{Pt-H} = 114.3, 1H, H^a], 7.41 [d, ³J_{H-H} = 7.33, 1H, H²], 7.31 [t, b, ³J_{H-H} = 8.36 Hz, 1H, H⁴], 7.27-7.22 [m, 1H, H³], 7.21-7.16 [m, 1H, H⁴], 7.15 [d, ³J_{H-H} = 7.77 Hz, 2H, H^{3,5}], 3.52 [s, ³J_{Pt-H} = 24.21, H^d], 3.29 [hept, 2H, H^b], 1.30 [d, ³J_{H-H} = 6.79 Hz, 6H, H^c], 1.12 [d, ³J_{H-H} = 6.87 Hz, 6H, H^c]. ¹³C NMR (CDCl₃): δ = 181.05 [s, C^a], 179.94 [s, C¹], 141.74 [s, C^{2,6}], 133.94 [s, C⁵], 133.58 [s, C⁴], 131.58 [s, C¹], 129.64 [s, C²], 128.11 [s, C³], 124.24 [s, C⁶], 124.73 [s, C⁴], 123.02 [s, C^{3,5}], 46.78 [s, C^d], 28.17 [s, C^b], 24.44 [s, C^c], 22.74 [s, C^c]. EI-MS: *m/z* 541.2 [M-OMe]⁺, 500.02 [M-Pr-2Me]⁺, 457.1 [M-Cl-dmso]⁺. Anal. Found (calc. for C₂₁H₂₈CINOPTS): C: 44.43 (44.01), H: 4.58 (4.92), N: 2.03 (2.44), S: 5.82 (5.60).

2a was obtained from compound **1** (0.062 g, 1.09 mmol) and 1,1'-bis(diphenylphosphino)-ferrocene (dppf) (0.030 g, 0.504 mmol) which were allowed to react in acetone (10 ml) at room temperature for 4 h. The solvent was removed on a rotary evaporator, yielding an orange solid which was dried in *vacuo*. Yield 65 mg (83%). M.p.: 184 -187 °C. IR (KBr): ν (CH=N) 1604 cm⁻¹. ¹H NMR (400 MHz, CDCl₃): δ = 8.17 [d, ⁴J_{Pt-H} = 9.54 Hz, ³J_{Pt-H} = 82.74 Hz, 2H, Ha], 7.62 – 7.57 [m, 8H, Ph-H], 7.35 [d, ³J_{H-H} = 7.57 Hz, 2H, H²], 7.29 [d, ³J_{H-H} = 6.99 Hz, 4H, H^{3,5}], 7.21 – 7.16 [m, 12H, Ph-H], 7.15 [t, ³J_{H-H} = 5.61 Hz, 2H, H⁴], 6.97 [t, ³J_{H-H} = 7.31 Hz, 2H, H³], 6.66 [dd, ³J_{H-H} = 7.94 Hz, ⁴J_{H-H} = 1.25 Hz, 2H, H⁴], 6.45 [dd, ³J_{H-H} = 7.92 Hz, ⁴J_{H-H} = 2.31 Hz, 2H, H⁵], 4.98 [s, 4H, Cp-H^a], 4.39 [s, 4H, Cp-H^b], 3.37 [hept, 4H, H^b], 1.30 [d, ³J_{H-H} = 6.76 Hz, 12H, H^c], 1.12 [d, ³J_{H-H} = 6.85 Hz, 12H, H^c]. ¹³C NMR (101 MHz, CDCl₃): δ = 179.47 [d, *J*_{Pt-C} = 3.07 Hz, *J*_{Pt-C} = 79.31 Hz, C^a], 146.60 [s, C¹], 141.83 [s, C^{2,6}], 137.36 [d, *J*_{Pt-C} = 4.36 Hz, *J*_{Pt-C} = 92.23 Hz, C⁵], 134.33 [d, *J*_{Pt-C} = 10.78 Hz, 8H, Ph-C], 132.00 [s, C⁴], 131.75 [s, C¹], 130.39 [s, C^{3,5}], 129.17 [s, C²], 127.57 [d, *J*_{Pt-C} = 11.01 Hz, 12H, Ph-C], 127.28 [s, C⁶], 122.92 [s, C³], 122.63 [s, C⁴], 76.73 [d, *J*_{Pt-C} = 10.45 Hz, C^a], 75.48 [d, *J*_{Pt-C} = 7.67 Hz, C^b], 28.12 [s, C^b], 24.79 [s, C^c], 23.14 [s, C^c]. ³¹P NMR (162 MHz, CDCl₃): δ = 9.42 [s, *J*_{Pt-P} = 4239 Hz]. EI-MS: *m/z* 1549.4 [M+5H]⁺, 1508.4 [M-Cl]⁺. Anal. Found (calc. for C₇₂H₇₂Cl₂FeN₂P₂Pt₂): C, 56.17 (56.00); H, 4.89 (4.70); N, 1.72 (1.81).

2b was obtained from compound **1** (0.058 g, 1.012 mmol) and 1,1'-bis(diphenylphosphino)-ethane (dppe) (0.020 g, 0.506 mmol) which were allowed to react in acetone (10 ml) at room temperature for 4 h. The formed yellow precipitate was collected

which was dried in *vacuo*. Yield 38 mg (54%). M.p.: 298 -301 °C. IR (KBr): ν (CH=N) 1602 cm⁻¹. ¹H NMR (400 MHz, CDCl₃): δ = 8.23 [d, ⁴J_{Pt-H} = 9.00 Hz, ³J_{Pt-H} = 86.40 Hz, 2H, Ha], 7.99 – 7.80 [m, 8H, Ph-H], 7.34 [d, ³J_{H-H} = 7.57 Hz, 2H, H²], 7.30 [d, ³J_{H-H} = 6.99 Hz, 4H, H^{3,5}], 7.28 – 7.16 [m, 14H, Ph-H & H⁴], 6.95 [dt, ³J_{H-H} = 7.4 Hz, ⁴J_{H-H} = 0.9 Hz, 2H, H³], 6.61 [dt, ³J_{H-H} = 7.6 Hz, ⁴J_{H-H} = 1.25 Hz, 2H, H⁴], 6.43 [dd, ³J_{H-H} = 7.9 Hz, ⁴J_{H-H} = 1.3 Hz, 2H, H⁵], 3.42 [hept, 4H, H^b], 3.09 [d, ²J_{Pt-H} = 2.6 Hz, 4H, H^d], 1.3d [d, ³J_{H-H} = 6.8 Hz, 12H, H^c], 1.21 [d, ³J_{H-H} = 6.9 Hz, 12H, H^c]. ¹³C NMR (75 MHz, CDCl₃): δ = 179.02 [d, *J*_{Pt-C} = 1.4 Hz, C^a], 146.11 [s, C¹], 141.86 [s, C^{2,6}], 136.77 [d, *J*_{Pt-C} = 3.1 Hz, C⁵], 134.29 [t, *J*_{Pt-C} = 5.6 Hz, Ph-C], 132.45 [s, C⁴], 130.69 [s, C¹], 129.94 [s, C^{3,5}], 129.17 [s, C²], 128.34 – 128.00 [m, Ph-C], 127.34 [s, C⁶], 122.75 [s, C³], 122.70 [s, C⁴], 28.14 [s, C^b], 24.57 [s, C^c], 23.15 [s, C^c], 1.03 [s, C^d]. ³¹P NMR (121 MHz, CDCl₃): δ = 18.21 [s, *J*_{Pt-P} = 4226 Hz, *J* = 26.4 Hz (virtual coupling)]. EI-MS: *m/z* 1393.4 [M+Na]⁺, 857.3 {M-[PtCl(N^αC)-Cl]}⁺. Anal. Found (calc. for C₆₄H₆₈Cl₂N₂P₂Pt₂): C, 55.68 (55.37); H, 4.52 (4.94); N, 1.96 (2.02).

2c was obtained in a similar manner as **2a**. Yield 65 mg (83%). M.p.: 286 -288 °C. IR (KBr): ν (CH=N) 1605 cm⁻¹. ¹H NMR (300 MHz, CDCl₃): δ = 8.13 [d, ⁴J_{Pt-H} = 8.9 Hz, ³J_{Pt-H} = 88.8 Hz, 2H, Ha], 8.04 [m, 8H, Ph-H], 7.33 – 7.24 [m, 8H, H², H^{3,5}, H⁴], 7.24 – 7.06 [m, 12H, Ph-H], 6.88 [dt, ³J_{H-H} = 7.4 Hz, ⁴J_{H-H} = 0.9 Hz, 2H, H³], 6.55 [dt, ³J_{H-H} = 7.7 Hz, ⁴J_{H-H} = 1.6 Hz, 2H, H⁴], 6.21 [dd, ³J_{H-H} = 8.0 Hz, ⁴J_{H-H} = 1.2 Hz, 2H, H⁵], 5.25 [t, ²J_{Pt-H} = 13.0 Hz, 2H, H^d], 3.42 [hept, 4H, H^b], 1.46 [d, ³J_{H-H} = 6.8 Hz, 12H, H^c], 1.23 [d, ³J_{H-H} = 6.9 Hz, 12H, H^c]. ¹³C NMR (75 MHz, CDCl₃): δ = 178.12 [d, *J*_{Pt-C} = 1.5 Hz, C^a], 144.93 [s, C¹], 143.74 [s, C⁴], 140.69 [s, C^{2,6}], 135.77 [d, *J*_{Pt-C} = 4.7 Hz, *J*_{Pt-C} = 82.3 Hz, C⁵], 134.16 [t, *J*_{Pt-C} = 6.0 Hz, Ph-C], 131.01 [s, C³], 129.21 [m, Ph-C], 127.72 [s, C⁴], 126.70 [m, Ph-C], 126.43 [s, C²], 121.78 [s, C^{3,5}], 121.74 [s, C⁶], 27.11 [s, C^b], 23.69 [s, C^c], 22.05 [s, C^c], 21.83 [s, C^d]. ³¹P NMR (121 MHz, CDCl₃): δ = 11.62 [s, *J*_{Pt-P} = 4261 Hz, *J* = 23.8 Hz (virtual coupling)]. EI-MS: *m/z* 1338.37 [M-Cl]⁺, 843.26 {M-[PtCl(N^αC)]-Cl}⁺. Anal. Found (calc. for C₆₃H₆₆Cl₂N₂P₂Pt₂): C, 55.32 (55.06); H, 4.68 (4.84); N, 1.98 (2.04).

3a was obtained from compound **1** (0.058 g, 0.92 mmol) and 1,1'-bis(diphenylphosphino)-ferrocene (dppf) (0.051 g, 0.92 mmol) which were allowed to react in acetone (10 ml) at room temperature for 4 h. The solvent was removed on a rotary evaporator, yielding an orange solid which was recrystallized from DCM/Hexane and dried in *vacuo*. Yield 80 mg (83%). M.p.: 205 – 208 °C. IR: ν (CH=N) 1624 cm⁻¹ (KBr); 1622 cm⁻¹ (DCM solution). ¹H NMR (400 MHz, CDCl₃): δ = 9.16 [s, 1H, H^a], 8.04 [s, br, 4H, Ph-H], 7.93 – 7.83 [m, 4H, Ph-H], 7.74 [dt, ³J_{H-H} = 5.9 Hz, ⁴J_{H-H} = 2.9 Hz, 1H, H²], 7.65 – 7.52 [m, 4H, Ph-H], 7.45 [dt, ³J_{H-H} = 4.6 Hz, ⁴J_{H-H} = 2.3 Hz, 6H, Ph-H], 7.37 [dd, ³J_{H-H} = 10.3 Hz, ⁴J_{H-H} = 4.2 Hz, 4H, Ph-H], 7.31 [m, 1H, H⁵], 7.16 [dt, ³J_{H-H} = 8.5 Hz, ⁴J_{H-H} = 4.1 Hz, 8H, Ph-H], 7.10 [d, ³J_{H-H} = 7.0 Hz, 1H, H⁴], 6.88 [dt, ³J_{H-H} = 9.2 Hz, ⁴J_{H-H} = 4.2 Hz, 2H, H^{3,5}], 6.71 [dt, ³J_{H-H} = 5.4 Hz, ⁴J_{H-H} = 1.7 Hz, 2H, H^{3,4}], 4.67 [d, ³J_{Pt-H} = 7.8 Hz, 2H, Cp-H^a], 4.47 [s, br, 2H, Cp-H^b], 4.08 [d, ³J_{Pt-H} = 7.8 Hz, 2H, Cp-H^a], 3.53 [s, br, 1H, Cp-H^b], 3.36 [s, br, 1H, Cp-H^b], 3.04 [hept, 2H, H^b], 1.08 [dd, *J*_{H-H} = 36.9 Hz, ³J_{H-H} = 6.8 Hz, 12H, H^c]. ¹³C NMR (101 MHz, CDCl₃) δ 166.34 [d, *J*_{Pt-C} = 4.2 Hz, C^a], 164.61 [d, *J*_{Pt-C} = 9.0 Hz, C¹], 163.43 [d, *J*_{Pt-C} = 9.0 Hz, C¹],

151.02 [s, C^{2,6}], 139.72 [s, C⁶], 138.06 [s, Ph-C], 136.06 [d, J_{P-C} = 3.3 Hz, J_{Pt-C} = 61.6 Hz C⁵], 135.43 – 135.06 (m, Ph-C), 133.66 (d, J_{P-C} = 11.9 Hz, C⁴), 133.03 (d, J_{P-C} = 14.8 Hz, Ph-C), 132.64 [s, Ph-C], 132.16 (d, J_{P-C} = 12.6 Hz, Ph-C), 131.69 (d, J_{P-C} = 7.7 Hz, Ph-C), 131.13 [s, Ph-C], 130.37 (d, J_{P-C} = 25.8 Hz, Ph-C), 129.80 (d, J_{P-C} = 7.0 Hz, C⁴), 128.37 (dd, J_{P-C} = 10.0, 3.6 Hz, Ph-C), 128.07 (d, J_{P-C} = 11.4 Hz, Ph-C), 127.58 (d, J_{P-C} = 11.2 Hz, C^{3,5}), 127.25 (d, J_{P-C} = 6.6 Hz, C²), 123.15 [s, C³], 122.66 [s, Ph-C], 76.15 (d, J_{P-C} = 12.9 Hz, Fc-C^α), 75.83 (d, J_{P-C} = 5.3 Hz, C^d), 75.66 (d, J_{P-C} = 10.9 Hz, Fc-C^α), 75.16 (d, J_{P-C} = 5.2 Hz, C^c), 74.94 (d, J_{P-C} = 6.7 Hz, Fc-C^β), 74.72 (d, J_{P-C} = 9.2 Hz, Fc-C^β), 74.04 (d, J_{P-C} = 8.5 Hz, Fc-C^β), 73.69 (d, J_{P-C} = 7.7 Hz, Fc-C^β), 72.71 (d, J_{P-C} = 5.8 Hz, Fc-C^α), 71.97 (d, J_{P-C} = 5.0 Hz, Fc-C^α), 27.87 [s, C^b], 23.81, 23.44 [ds, C^{c,c}]. ³¹P NMR (121 MHz, CDCl₃): δ = 15.74 [d, J_{P-P} = 15.9 Hz, J_{P-Pt} = 1704.9, P_B], 14.89 [d, J_{P-P} = 15.9 Hz, J_{P-Pt} = 4353.0 Hz, P_A]. EI-MS: *m/z* 1013.2 [M-Cl]⁺. Anal. Found (calc. for C₅₃H₅₀ClFeNP₂Pt): C, 61.14 (60.67); H, 4.67 (4.80); N, 1.35 (1.33).

3b was obtained from compound **1** (0.050 g, 0.087 mmol) and bis(diphenylphosphino)ethane (dppe) (0.035 g, 0.087 mmol) which were allowed to react in acetone (10 ml) at room temperature for 4 h. The solvent was removed on a rotary evaporator, and the residue obtained was dissolved in a minimum amount of CH₂Cl₂ and passed through a SiO₂ column. Elution with an n-hexane/ethyl acetate (50:50) mixture removed the impurities and the product band was eluted using methanol. The yellow solid obtained was recrystallized from acetone giving an off white crystalline solid. Yield 33 mg (42%). M.p.: 320 – 323 °C. IR: ν (CH=N) 1631 cm⁻¹ (KBr); 1602 cm⁻¹ (DCM solution). ¹H NMR (300 MHz, CDCl₃): δ = 8.28 [d, ⁴J_{H-P} = 8.09 Hz, ³J_{Pt-H} = 83.82 Hz, 1H, H^a], 7.94 [dd, ³J_{H-P} = 11.98 Hz, ³J_{H-H} = 7.56 Hz, 4H, Ph-H], 7.60 - 7.52 [m, 8H, Ph-H], 7.39 [m, 2H, Ph-H], 7.30 – 7.20 [m, 7H, H³ and 6 Ph-H], 7.15 [t, ³J_{H-H} = 7.69 Hz, 1H, H⁴], 7.01 [t, ³J_{H-H} = 7.77 Hz, 1H, H⁴], 6.98 – 6.88 [m, 2H, H^{2,5}], 6.78 [d, ³J_{H-H} = 7.79 Hz, 2H, H^{3,5}], 3.08 [hept, 2H, H^b], 2.58 [dt, ²J_{P-H} = 27.06 Hz, ³J_{H-H} = 14.78 Hz, 2H, H^e], 2.30 [dt, ²J_{P-H} = 21.88 Hz, ³J_{H-H} = 13.64 Hz, 2H, H^d], 0.95, 0.53 [ds, br, 12H, H^{c,c}]. ¹³C NMR (CDCl₃): δ = 184.92 [s, b, C^a], 163.30 [dd, J_{Pcis-C} = 5.62 Hz, J_{Ptrans-C} = 105.58 Hz, C⁶], 147.20 [d, J_{Pcis-C} = 8.29 Hz, C¹], 140.26 [s, C^{2,6}], 138.51 [d, J_{Pcis-C} = 3.19 Hz, J_{Pt-C} = 90.59 Hz, C⁵], 134.16 [d, J_{P-C} = 13.67 Hz, Ph-C], 133.05 [d, J_{P-C} = 11.12 Hz, Ph-C], 132.78 [d, J_{P-C} = 2.03 Hz, C³], 131.49 [d, J_{P-C} = 1.96 Hz, Ph-C], 130.02 [d, J_{P-C} = 4.00 Hz, C¹], 129.49 [dd, J_{P-C} = 13.67, 22.46 Hz, Ph-C], 128.67 [s, P-C], 128.33 [s, C⁴], 128.21 [s, P-C], 126.23 [s, C⁴], 125.92 [s, P-C], 125.31 [s, P-C], 123.74 [s, C^{3,5}], 29.08 [m, C^{e,d}], 28.15 [s, C^b], 25.46, 21.80 [ds, b, C^{c,c}]. ³¹P NMR (121 MHz, CDCl₃): δ = 43.30 [s, J_{P-Pt} = 1900.91, P_B], 39.65 [s, J_{P-Pt} = 3711.14, P_A]. EI-MS: *m/z* 857.28 [M-Cl]⁺. Anal. Found (calc. for C₄₅H₄₆ClNP₂Pt): C, 60.32 (60.50); H, 5.23 (5.19); N, 1.46 (1.57).

3c was obtained from compound **1** (0.050 g, 0.087 mmol) and bis(diphenylphosphino)ethane (dppe) (0.035 g, 0.087 mmol) which were allowed to react in acetone (10 ml) at room temperature for 4 h. The solvent was removed on a rotary evaporator, and dried in *vacuo* to give a dark yellow oil. Yield 33 mg (42%). IR: ν (CH=N) 1599 cm⁻¹ (KBr); 1601 cm⁻¹ (DCM solution). ¹H NMR (300 MHz, CDCl₃): δ = 8.28 [d, ⁴J_{H-P} = 8.1 Hz, ³J_{Pt-H} = 86.1 Hz, 1H, H^a], 8.00 – 7.87 [m, 4H, Ph-H], 7.66 –

7.49 [m, 6H, 4Ph-H & H^{3,4}], 7.39 – 7.31 [m, 3H, 2Ph-H & H⁴], 7.31 – 7.22 [m, 2H, H^{2,5}], 7.17 [dt, ³J_{H-P} = 7.8 Hz, ³J_{H-H} = 2.8 Hz, 4H, Ph-H], 7.13 – 7.02 [m, 8H, 6Ph-H & H^{3,5}], 4.85 [dd, ³J_{H-P} = 12.0 Hz, ³J_{H-H} = 9.3 Hz, 2H, H^d], 3.29 [hept, 2H, H^b], 1.05, 0.57 [ds, br, 12H, H^{c,c}]. ¹³C NMR (101 MHz, CDCl₃): δ = 183.86 [s, b, C^a], 160.48 [s, C¹], 159.38 [s, C¹], 147.89 [s, C^{2,6}], 147.35 [s, C⁶], 140.94 [d, J_{P-C} = 1.3 Hz, Ph-C], 138.48 – 138.07 (m, Ph-C), 134.79 [m, Ph-C], 134.00 (d, J_{P-C} = 12.6 Hz, Ph-C), 133.14 [s, C³], 133.02 (d, J_{P-C} = 12.8 Hz, Ph-C), 131.85 (d, J_{P-C} = 2.7 Hz, Ph-C), 130.29 [s, C⁴], 129.70 (dd, J_{P-C} = 27.6, 11.6 Hz, Ph-C), 128.47 [s, C²], 128.10 (d, J_{P-C} = 5.0 Hz, Ph-C), 127.69 (d, J_{P-C} = 5.1 Hz, Ph-C), 126.81 [s, C⁵], 124.53 [s, C⁴], 124.45 [s, C^{3,5}], 43.63 [t, C^d], 28.44 [s, C^b], 25.49 [s, C^c], 21.99 [s, C^c]. ³¹P NMR (121 MHz, CDCl₃): δ = -28.33 [d, J_{P-P} = 40.12 Hz, J_{P-Pt} = 1463.6 Hz, P_B], -31.96 [d, J_{P-P} = 40.13 Hz, J_{P-Pt} = 3316.8 Hz, P_A]. EI-MS: *m/z* 843.2 [M-Cl]⁺. Anal. Found (calc. for C₄₄H₄₄ClNP₂Pt): C, 60.28 (60.10); H, 4.96 (5.04); N, 1.48 (1.59).

4.3. Variable Temperature NMR study

A J-Young valved NMR tube was charged with cationic complex **3a** (20 mg, 0.0190 mmol) and CDCl₃ (0.7 ml). After purging with argon the complex solution was frozen at -196 °C and subjected to three freeze-pump-thaw cycles to remove any dissolved oxygen. ³¹P NMR spectrum was recorded in the temperature range from -50 to 40 °C. Methanol was employed as a calibration standard.

4.4. Computational Methods

Hardware. The hardware used for the molecular modeling is the “Sun Hybrid System” based at the Centre of High Performance Computing (CHPC) in Cape Town, South Africa.

Software. All computational results in this study were calculated using the DMol³ density functional theory (DFT) code²⁰ as implemented in Accelrys MaterialsStudio (Version 5.5). The nonlocal generalized gradient approximation (GGA) exchange-correlation functional was employed in all geometry optimizations, viz., the PW91 functional of Perdew and Wang.²¹ An all-electron polarized split valence basis set, termed double numeric polarized (DNP), has been used. All geometry optimizations employed highly efficient delocalized internal coordinates.²² The tolerance for convergence of the self-consistent field (SCF) density was set to 1 x 10⁻⁵ hartrees, while the tolerance for energy convergence was set to 1 x 10⁻⁶ hartrees. Additional convergence criteria include the tolerance for converged gradient (0.002 hartrees/Å) and the tolerance for converged atom displacement (0.005 Å). The thermal smearing option in MaterialsStudio makes use of a fractional electron occupancy scheme at the Fermi level according to a finite-temperature Fermi function.^{21,23}

In all cases optimized geometries were subjected to full frequency analyses at the same GGA/PW91/DNP level of theory to verify the nature of the stationary points. Equilibrium geometries were characterized by the absence of imaginary frequencies. All calculations were performed with the incorporation of solvent effects (COSMO). All results were electron balanced for the isolated system in the gas phase. The reported relative Gibbs free energies refer to Gibbs free energy corrections to the total electronic energies at 298.15 K and 1 atm.

Acknowledgment

Acknowledgements go to National Research Foundation (South Africa) and the DST/NRF COE in Catalysis (c*change) for funding. This work was also supported by Research Committees of the University of Cape Town and Stellenbosch University.

Notes and references

^a Department of Chemistry, University of Cape Town, Private Bag, Rondebosch, 7700, South Africa.

^b Catalysis and Synthesis Research Group, Chemical Resource Beneficiation Focus Area, North-West University, Potchefstroom, 2520, South Africa

^c Department of Chemistry and Polymer Science, Stellenbosch University, Private Bag, Matieland, 7601, Stellenbosch, South Africa.

* Email: smapolie@sun.ac.za

† Electronic Supplementary Information (ESI) available: Additional Crystallographic data in CIF format and figures for IR spectra, UV spectra, tables for conductivity, UV data etc., as well as tables of structural refinement. Together with tables giving Cartesian coordinates for the calculated stationary structures obtained from the DFT calculations has been deposited as supplementary material. See DOI: 10.1039/b000000x/

Crystallographic data for complexes **2a**, **2c**, **3a** and **3b** can be found in the CCDC (reference numbers 928868 – 928871). This data can be obtained free of charge at www.ccdc.cam.ac.uk/conts/retrieving.html (or from the Cambridge Crystallographic Data Centre, 12, Union Road, Cambridge CB2 1EZ, U.K.; fax (internat.) +44-1223/336-033; email deposit@ccdc.cam.ac.uk).

1 J. Forniés, V. Sicilia, C. Larraz, J. A. Camerano, A. Martín, J. M. Casas and A. C. Tsipis, *Organometallics*, 2010, **29**, 1396.

2 (a) A. Capapé, M. Crespo, J. Granell, M. Font-Bardiab and X. Solans, *Dalton Trans.*, 2007, 2030; (b) A. Capapé, M. Crespo, J. Granell, A. Vizcarro, J. Zafrilla, M. Font-Bardía and X. Solans, *Chem. Commun.*, 2006, 4128.

3 (a) M. Strotmann, R. Wartchow and H. Butenschön, *ARKIVOC*, 2004, **xiii**, 57; (b) P. Teo, L. L. Koh, and T. S. A. Hor, *Chem. Commun.*, 2007, 4221.

4 (a) S. M. Nabavizadeh, H. Amini, H. R. Shahsavari, M. Namdar, M. Rashidi, R. Kia, B. Hemmateenejad, M. Nekoeinia, A. Ariafard, F. N. Hosseini, A. Gharavi, A. Khalafi-Nezhad, M. T. Sharbati and F. Panahi, *Organometallics*, 2011, **30**, 1466; (b) S. Jamali, S. M. Nabavizadeh and M. Rashidi, *Inorg. Chem.*, 2008, **47**, 5441; (c) H. Samoueia, M. Rashidia and F. W. Heinemann, *J. Organometal. Chem.*, 2011, **696**, 3764.

5 M. G. Haghigi, M. Rashidi, S. M. Nabavizadeh, S. Jamali and R. J. Puddephatt, *Dalton Trans.*, 2010, **39**, 11396.

6 M. Frezza, Q. P. Dou, Y. Xiao, H. Samouei, M. Rashidi, F. Samari and B. Hemmateenejad, *J. Med. Chem.*, 2011, **54**, 6166.

7 (a) J. Albert, M. Gómez, J. Granell, J. Sales and X. Solans, *Organometallics*, 1990, **9**, 1405; (b) J. Albert, J. Granell, J. Sales, M. Font-Bardía and X. Solans, *Organometallics*, 1995, **14**, 1393; (c) M. Crespo, X. Solans and M. Font-Bardía, *Organometallics*, 1995, **14**, 355; (d) M. Crespo, J. Granell, X. Solans and M. Font-Bardía, *J. Organomet. Chem.*, 2003, **681**, 143.

8 (a) R. Martín, M. Crespo, M. Font-Bardía and T. Calvet, *Polyhedron*, 2009, **28**, 1369; (b) P. S. Pregosin and R. W. Kunz, in: Diehl, P.; Fluck, E.; Kosfeld, R. (Eds.), *³¹P and ¹³C NMR of Transition Metal Phosphine Complexes*, Springer-Verlag, Berlin, **1979**.

9 P. W. Cyr, B. O. Patrick and B. R. James, *Chem. Commun.*, 2001, 1570.

10 M. J. Cowley, J. M. Lynam, R. S. Moneypenny, A. C. Whitwood and A. J. Wilson, *Dalton Trans.*, 2009, 9529.

11 G. Bandoli and A. Dolmella, *Coord. Chem. Rev.*, 2000, **209**, 161.

12 J.-F. Ma and Y. Yamamoto, *Inorg. Chim. Acta*, 2000, **299**, 164.

13 (a) B. D. Swartz and C. Nataro, *Organometallics*, 2005, **24**, 2447; (b) C. Nataro, A. N. Campbell, M. A. Ferguson, C. D. Incarvito and A. L. Rheingold, *J. Organometal. Chem.* 2003, **673**, 47.

14 (a) S. Fernández, J. Forniés, B. Gil, J. Gómez and E. Lalinde, *Dalton Trans.* 2003, 822; (b) S. W. Lai, H. W. Lam, W. Lu, K. K. Cheung and C. M. Che, *Organometallics*, 2002, **21**, 226; (c) P. Shao, Y. Li, A. Azenkeng, M. R. Hoffmann and W. Sun, *Inorg. Chem.*, 2009, **48**, 2407; (d) D. Qiu, J. Wu, Z. Xie, Y. Cheng and L. Wang, *J. Organomet. Chem.*, 2009, **694**, 737.

15 (a) A. Díez, J. Forniés, S. Fuertes, E. Lalinde, C. Larraz, J. A. López, A. Martín, M. T. Moreno and V. Sicilia, *Organometallics*, 2009, **28**, 1705; (b) J. Schneider, P. Du, P. Jarosz, T. Lazarides, X. Wang, W. W. Brennessel and R. Eisenberg, *Inorg. Chem.*, 2009, **48**, 4306; (c) J. Brooks, Y. Babayan, S. Lamansky, P. I. Djurovich, I. Tsyba, R. Bau and M. E. Thompson, *Inorg. Chem.*, 2002, **41**, 3055; (d) J. Schneider, P. Du, X. Wang, W. W. Brennessel and R. Eisenberg, *Inorg. Chem.*, 2009, **48**, 1498.

16 Z. Otwinowski and W. Minor, *Methods in Enzymology, Macromolecular Crystallography*, C. W. Carter Jr, & R. M. Sweet, Eds., part A, 1997, **276**, 307-326, Academic Press.

17 G. M. Sheldrick, SADABS, University of Göttingen, Germany, 1996.

18 G. M. Sheldrick, SHELXL-97 and SHELXS-97, University of Göttingen, Germany, 1997.

19 L. J. Barbour, *J. Supramol. Chem.*, 2001, **1**, 189.

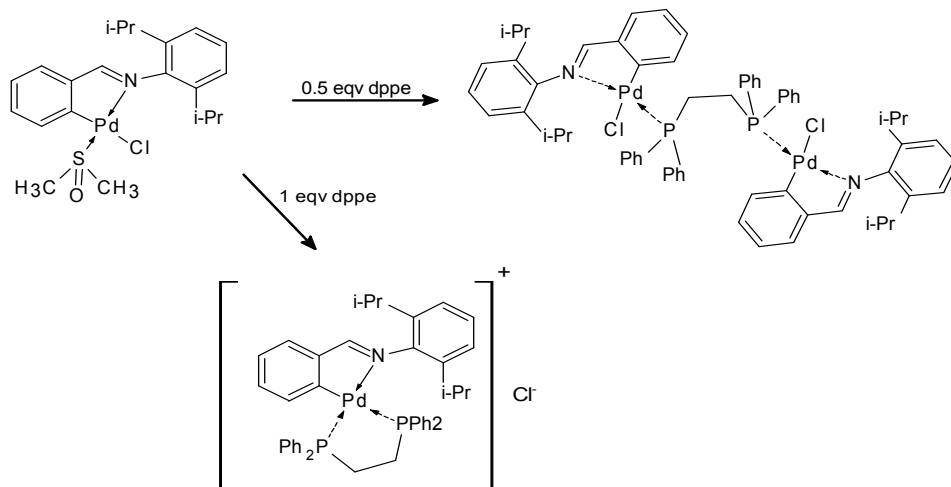
20 (a) B. Delley, *J. Chem. Phys.*, 1992, **92**, 508; (b) B. Delley, *J. Phys. Chem.*, 1996, **100**, 6107; (c) B. Delley, *J. Chem. Phys.*, 2000, **113**, 7756.

21 J. P. Perdew and Y. Wang, *Phys. Rev. B* **1992**, **45**, 13244-13249.

22 J. Andzelm, R. D. King-Smith and G. Fitzgerald, *Chem. Phys. Lett.*, 2001, **335**, 321.

23 M. Weinert and J. W. Davenport, *Phys. Rev. B*, 1992, **45**, 13709.

TOC graphical abstract



The reaction of the cyclometallated complex $[\text{PdCl}(\text{N}^{\wedge}\text{C})(\text{dmsf})]$ **1**, ($\text{N}^{\wedge}\text{C}$ represents the cyclometallated Schiff base, benzylidene-2,6-diisopropylphenylamine), with 1,1-bis(diphenylphosphino)ferrocene, dppe, 1,1-bis(diphenylphosphino)methane, dppf, and 1,2-bis(diphenylphosphino)ethane, dppe, in a 2:1 ratio or an equimolar ratio using acetone as solvent produced the corresponding binuclear and mononuclear diphosphine platinum complexes